MULTI-QUASIPARTICLE HIGH-K STATES AND THEIR ROTATIONS*

F.R. Xu[a,b], X.M. Fu[a], W.Y. Liang[a], Y. Shi[a], H.L. Liu[c]
P.M. Walker[d]

[a]State Key Laboratory of Nuclear Physics and Technology, School of Physics
Peking University, Beijing 100871, China
[b]State Key Laboratory of Theoretical Physics, Institute of Theoretical Physics
Chinese Academy of Sciences, Beijing 100190, China
[c]Department of Applied Physics, Xi'an Jiaotong University, Xi'an 710049, China
[d]Department of Physics, University of Surrey, Guildford GU2 7XH, UK

(Received November 10, 2015)

Based on the Woods–Saxon potential, we have developed a configuration-constrained potential energy surface calculation. This method has been successfully applied to the calculations of various multi-quasiparticle high-K states in different mass regions, well reproducing the experimental excitation energies and other observations. Further, we have developed the configuration-constrained total Routhian surface calculation for the rotations of the multi-quasiparticle high-K states. The pairing calculation is improved by a particle-number-conserving pairing method which always gives converged solutions for the cranking Hartree–Fock pairing calculations. In this paper, we focus on the predictions of possible octupole deformed high-K states in the actinide mass region. Using the developed configuration-constrained total Routhian surface method, we have investigated high-K rotations for nuclei around $Z = 100$ and 102 with $N \approx 150$.

DOI:10.5506/APhysPolBSupp.8.715
PACS numbers: 21.10.–k, 21.60.Cs, 23.20.Lv

1. Introduction

Atomic nuclei can be excited by breaking paired nucleons [1–4]. If the unpaired nucleons couple to a configuration with a high angular momentum (in fact, an angular momentum projection onto the symmetry axis of a deformed nucleus, named K), the excited state can be an isomer due to the forbiddenness of electromagnetic decays from high-K to low-K states [1, 2]. An abundance of high-K isomers have been observed in the whole chart of nuclides [1, 2] including superheavy (see Ref. [5] and references therein) and nuclei near drip lines [6, 7].

* Presented at the XXII Nuclear Physics Workshop "Marie and Pierre Curie", Kazimierz Dolny, Poland, September 22–27, 2015.

Theoretically, previous calculations were usually done with the assumption that an isomer has the same deformation as the ground state of the nucleus (see, *e.g.*, [8]). However, high-Ω orbits (Ω is the nucleon angular momentum projection onto the symmetry axis of the deformed nucleus) usually have a strong deformation-driving force, which would make the isomer shape deviate from that of the ground state. Particularly for soft nuclei, the deformation change can be remarkable due to the broken-pair excitations [9–13]. The multi-quasiparticle excitations even lead to the emergence of new deformation degrees of freedom [14]. The deformation evolution can also occur due to collective rotations of nuclear states [3, 10, 15], and the broken-pair multi-quasiparticle high-K states can have collective rotations. The rotational bands built on multi-quasiparticle configurations are called sidebands (relative to the ground-state band), providing rich information for nuclear structure studies. Theoretically, the calculations of sidebands are difficult due to the non-convergence problem in the cranking Hartree–Fock–Bogoliubov (HFB) calculation. In this paper, we discuss multi-quasiparticle high-K states and their collective rotations.

2. Model

The deformed Woods–Saxon (WS) potential with the universal parameters [16] gives an excellent single-particle level spacing that is crucial for quantitative calculations of excitation energies of broken-pair multi-quasiparticle high-K states. The pairing is another crucial factor for the energy calculations. In the present calculations, only the monopole pairing is considered. It was found that quadrupole pairings [17] have only a small effect on the excitation energy calculations of multi-quasiparticle states [18]. The BCS pairing provides a simple and efficient model for non-rotational calculations. In the present calculations, in order to avoid the spurious phase transition encountered in the BCS approach, we used the approximate particle number projection by means of the Lipkin–Nogami (LN) pairing method. In the macroscopic–microscopic model, the total energy of a state contains a macroscopic part that is calculated by the liquid drop model and a microscopic part that can be obtained by the Strutinsky shell correction. The configuration energy in the LN approach can be written as [3]

$$\begin{aligned} E_{\mathrm{LN}} &= \sum_{j=1}^{S} e_{k_j} + \sum_{k\neq k_j} 2V_k^2 e_k - \frac{\Delta^2}{G} - G\sum_{k\neq k_j} V_k^4 \\ &\quad + G\frac{N-S}{2} - 4\lambda_2 \sum_{k\neq k_j} (U_k V_k)^2 \,, \end{aligned} \tag{1}$$

where S is the seniority of the given type of nucleon, *i.e.*, the number of unpaired protons or neutrons (indicated by k_j), and N is the number of protons or neutrons. Adiabatic blockings are achieved by tracking the specific single-particle orbits using calculated average Nilsson numbers which evolve smoothly with changing deformation [3]. In the non-axial deformed Woods–Saxon potential, the Nilsson numbers $\Omega[N, n_z, \Lambda]$ of single-particle orbits are no longer good quantum numbers, but we can calculate their expectation (averaged) values by using single-particle wavefunctions. The expectation values are approximately good quantum numbers when deformations are nearly prolate or oblate.

The PES is calculated usually with deformations (β_2, γ, β_4). The total energy of a state is obtained by minimizing the calculated PES. The excitation energy of the state is given by the total energy difference between the excited and ground states. In many cases, high-K states have axial deformed shapes (prolate or oblate [19]). An axially-symmetric shape leads to a conserved K value. In some cases (particularly in heavy mass regions), however, higher-order deformations may need to be considered, *e.g.*, β_6 and β_8, or reflection-asymmetric octupole deformation β_3 [14, 20, 21]. The γ deformation can also play an important role in the description of nuclear collective rotation [17, 22, 23] and high-K excitations [24–28]. The γ deformation results in K mixing [29–31]. The pairing strength is readjusted by including mean-field and blocking effects [32]. In the usual BCS pairing, the pairing gap is assumed to be equal to the experimental odd–even mass difference, which is used to determine the pairing strength. But in Refs. [32, 33], it was pointed out that the three-point or four-point (even five-point) odd–even mass difference formula cannot fully cancel effects from the mean field itself and the odd-nucleon blocking. The twofold degeneracy of single-particle levels can lead to a contribution to the odd–even mass difference [33]. The neighbouring nuclei involved in the odd–even mass difference calculation may have different deformations, which can affect the odd–even difference [32]. In the present readjustment, we use a five-point odd–even mass difference formula to calculate a theoretical odd–even mass difference, and adjust the pairing strength to reproduce the experimental odd–even mass difference [32]. The readjustment is crucial for the calculations of excitation energies.

The multi-quasiparticle high-K states can undergo collective rotations. For collective rotational calculations, the total Routhian surface (TRS) method has been very successful. The shape evolution with increasing rotational frequency can be obtained by minimizing the calculated TRS. However, for broken-pair multi-quasiparticle states, the cranking Hartree–Fock–Bogoliubov (HFB) approach which was used in the conventional TRS calculation encounters a non-convergence problem [34, 35]. In order to overcome the problem, we have developed the total Routhian surface method by incorporating the particle-number-conserving (PNC) pairing method [36].

The total Routhian can be written as [37]

$$E^{\omega}\left(Z,N,\hat{\beta}\right) = E^{\omega=0}\left(Z,N,\hat{\beta}\right) + \left[\left\langle \hat{H}^{\omega}\left(Z,N,\hat{\beta}\right)\right\rangle - \left\langle \hat{H}^{\omega=0}\left(Z,N,\hat{\beta}\right)\right\rangle\right] . \quad (2)$$

The notations are standard, see Ref. [37] for details. The cranked shell-model Hamiltonian is written as [34–36]

$$H_{\rm CSM} = H_{\rm SP} - \omega J_x + H_{\rm P} , \quad (3)$$

where $H_{\rm SP} = \sum_{\xi} h_{\xi}$ with h_{ξ} being the single-particle Hamiltonian with a one-body potential. $-\omega J_x = -\omega \sum j_x$ is the Coriolis energy (j_x for the single-particle spin projection onto the x axis, perpendicular to the symmetry axis), and $H_{\rm P}$ is the residual two-body pairing interaction,

$$H_{\rm P} = -G \sum_{\xi\eta} a^{\dagger}_{\xi} a^{\dagger}_{\bar{\xi}} a_{\bar{\eta}} a_{\eta} , \quad (4)$$

where ξ ($\bar{\xi}$) and η ($\bar{\eta}$) index the (time-reversed) eigenstates of the single-particle Hamiltonian, h_{ξ}. In the rotational case, the time-reversed symmetry is broken, while the signature α, defined by $R_x(\pi)|\xi\alpha\rangle = e^{-i\pi\alpha}|\xi\alpha\rangle$, remains a good quantum number. One can transform the time-reversed representation into the signature basis by [34–36]

$$\beta^{\dagger}_{\xi\alpha=\pm 1/2} = \frac{1}{\sqrt{2}}\left\{a^{\dagger}_{\xi} \pm \pi a^{\dagger}_{-\xi}\right\} , \quad (5)$$

where $a^{\dagger}_{-\xi} = (-1)^{\Omega-1/2} a^{\dagger}_{\bar{\xi}}$ with Ω being the single-particle spin projection onto the symmetry axis. The parity π stays conserved. Then, we have

$$H_{\rm P} = -G \sum_{\xi\eta} (-1)^{\Omega_{\xi}-\Omega_{\eta}} \beta^{\dagger}_{\xi+} \beta^{\dagger}_{\xi-} \beta_{\eta-} \beta_{\eta+} , \quad (6)$$

where $\xi+$ ($\xi-$) indicates the eigenstate ξ with positive (negative) signature [34–36].

The eigenstates $|\mu\alpha\rangle$ of the cranked single-particle Hamiltonian, $h_{\xi} - \omega j_x$, can be expressed as

$$|\mu\alpha\rangle = \sum_{\xi} c_{\mu\xi}(\alpha)|\xi\alpha\rangle \quad [c_{\mu\xi}(\alpha) \text{ is real}] , \quad (7)$$

where $|\xi\alpha\rangle$ stands for the eigenstates of the non-cranked single-particle Hamiltonian, h_{ξ}, while the signature α is conserved. The coefficients $c_{\mu\xi}(\alpha)$

are determined in the diagonalization of the $h_\xi - \omega j_x$ Hamiltonian in the signature basis of the h_ξ Hamiltonian. Correspondingly, a cranked many-particle configuration of the n-body system can be written as a product form

$$|\mu_1\mu_2\cdots\mu_n\rangle = b^\dagger_{\mu_1} b^\dagger_{\mu_2}\cdots b^\dagger_{\mu_n}|0\rangle\,, \tag{8}$$

where $b^\dagger_{\mu_i}$ is the creation operator for a cranked single-particle state $|\mu_i\alpha\rangle$. (In fact the eigen state $|\mu\alpha\rangle$ contains other quantum numbers, *e.g.*, eigen energy $\varepsilon_{\mu\alpha}$ and parity π, but it is sometimes denoted by μ for simplification hereafter.) According to Eq. (7), we have

$$b^\dagger_{\mu\pm} = \sum_\xi c_{\mu\xi}(\pm)\beta^\dagger_{\xi\pm}\,, \tag{9}$$

where the sign $\pm$ indicates positive or negative signature. In the cranked basis, therefore, the residual two-body paring interaction can be written as [36]

$$H_{\rm P} = -G\sum_{\mu\mu'\nu\nu'} f^*_{\mu\mu'} f_{\nu\nu'} b^\dagger_{\mu+} b^\dagger_{\mu'-} b_{\nu-} b_{\nu'+}\,, \tag{10}$$

with

$$f^*_{\mu\mu'} = \sum_{\xi\xi'} e^{i\pi\Omega_\xi} c_{\mu\xi}(+) c_{\mu'\xi'}(-)\,, \tag{11}$$

$$f_{\nu\nu'} = \sum_{\eta\eta'} e^{-i\pi\Omega_\eta} c_{\nu\eta}(+) c_{\nu'\eta'}(-)\,. \tag{12}$$

The eigenstate of $H_{\rm CSM}$ can be written as [34–36]

$$\left|\psi^\omega_{\rm CSM}\right\rangle = \sum_i C_i|i\rangle\,, \tag{13}$$

with $\{|i\rangle;\, i = 1, 2, \cdots\} = \{|\mu_1\mu_2\cdots\mu_n\rangle;\, \text{scanning}\}$, taking all possible configurations in the truncated CMPC space. For more details, see Refs. [34–36].

The total cranked shell-model Hamiltonian, $H_{\rm CSM}$, is diagonalized in a cranked many-particle configuration (CMPC) model space, *i.e.*, one chooses the eigenstates of the no-pairing cranked deformed Hamiltonian as basis functions for the diagonalization of the total cranked Hamiltonian, $H_{\rm CSM}$ [36]. The cranked deformed basis provides a small but efficient model space for the PNC pairing calculations [34, 35].

The angular momentum of the rotational state $|\psi^\omega_{\rm CSM}\rangle$ is calculated by [36]

$$\langle\psi^\omega_{\rm CSM}|\, J_x\, |\psi^\omega_{\rm CSM}\rangle = \sum_i C_i^2\langle i|J_x|i\rangle + 2\sum_{i<j} C_i C_j\langle i|J_x|j\rangle\,. \tag{14}$$

The TRS is calculated in a lattice of deformations (β_2, γ, β_4). The γ deformation can play an important role in the description of nuclear collective rotation [17, 22, 23] and high-K excitations [24–28], leading to K mixing [29–31]. The configuration-constrained calculation is achieved by identifying and tracking the given single-particle orbits using calculated average Nilsson numbers. The specific orbits define the multi-quasiparticle high-K configuration.

In this paper, we have introduced two different models. The configuration-constrained PES model with the Lipkin–Nogami pairing is only for the calculations of multi-quasiparticle states without collective rotations, *i.e.*, the bandheads of their rotational bands. The configuration-constrained TRS with the PNC pairing is for the collective rotational calculations of the excited configurations. Of course, the TRS method is also valid for the bandhead calculations. In the two models, the one-body Hamiltonian $H_{\rm SP}$ takes the same form, with the universal Woods–Saxon parameters [16]. The residual two-body pairing interaction $H_{\rm P}$ is also identical. However, the pairing strengths are different. The pairing strength is dependent on both the model itself and the model space. Nevertheless, it is required to reproduce the experimental odd–even mass difference. For the nuclei investigated in the present paper, we took an equal number of about 40 single-particle levels above and below the Fermi surface for the Lipkin–Nogami pairing. The pairing strength is obtained by the averaged gap method [38]. In the PNC calculations, the model dimension taken for the Hamiltonian diagonalization is about 1000. It has been well tested that such a dimension is sufficient for converged solutions, see Refs. [34,35] for details. The PNC pairing strength is determined also by fitting the experimental odd–even mass difference [34,35]. The resulting pairing energies are similar for the Lipkin–Nogami and PNC calculations. For example, in the ^{178}W $K^\pi = 7^-$, $\nu 7/2^+[633] \otimes \nu 7/2^-[514]$ state (at $\hbar\omega = 0.0$ MeV), the calculated pairing energy is -1.9 MeV in the Lipkin–Nogami calculation, compared with -2.5 MeV with PNC [34].

3. Calculations

We have investigated multi-quasiparticle high-K states in different mass regions. The PES calculations can give excitation energies, deformations, g-factors, and softness as well. Figure 1 displays the calculated configuration-constrained PESs for the for the prolate $K^\pi = 6^-$ ($\nu\{7/2[633], 5/2[512]\}$) and the oblate $K^\pi = 11^-$ ($\pi\{13/2[606], 9/2[505]\}$) states in ^{186}Pb. We see that the $K^\pi = 6^-$ isomer has a soft prolate shape, while the $K^\pi = 11^-$ isomer has a oblate shape, making shape coexistence in this nucleus [39].

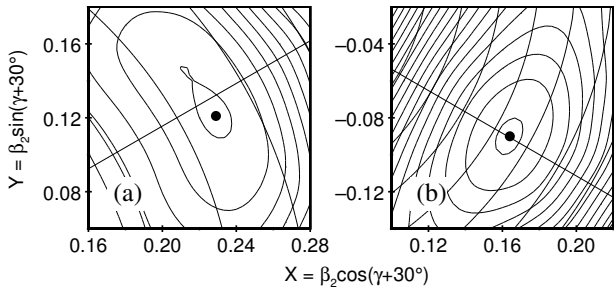

Fig. 1. Configuration-constrained PESs for the *prolate* $K^\pi = 6^-(\nu\{7/2[633], 5/2[512]\})$ state (a) and the *oblate* $K^\pi = 11^-(\pi\{13/2[606], 9/2[505]\})$ state (b) in ^{186}Pb. The energy difference between neighboring contours is 100 keV. The intrinsic PESs are reflection-symmetric about $\gamma = 0°$; that is, the shape with $\gamma = -60°$ is the same as the one with $\gamma = 60°$ for non-collective excitations.

We have searched for possible octupole deformed high-K states in the actinide region. The calculations were performed in multi-dimensional deformation space $(\beta_2, \beta_3, \beta_4, \beta_5)$ [14]. Figure 2 plots the calculated configuration-constrained PESs for two-quasiparticle $K^\pi = 6^-$ states in ^{232}Th, ^{234}U and ^{236}Pu, showing octupole deformations or octupole softness. Experiments have observed a $K^\pi = 6^-$ isomer at an excitation energy of 1.42 MeV with $T_{1/2} = 33.5$ μs in 234U [40]. The experimental energy is reproduced by the present calculation giving $E_x = 1.26$ MeV.

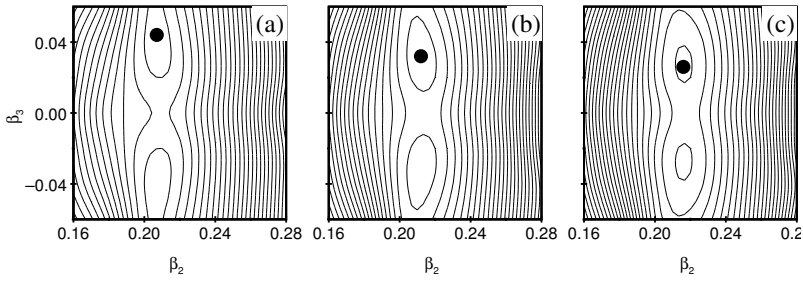

Fig. 2. Calculated PESs of $K^\pi = 6^-(\nu\{5/2^+[633]\otimes 7^-/2[743]\})$ states for (a) ^{232}Th, (b) ^{234}U, and (c) ^{236}Pu. At each (β_2, β_3) deformation point, the energy has been minimized with respect to β_4 and β_5 deformations. The energy interval between neighboring contours is 100 keV. The PES is symmetric with respect to $\beta_3 = 0$.

Using the configuration-constrained cranking TRS method [34, 35], we have investigated the collective rotations of multi-quasiparticle high-K states. Figure 3 shows the calculated kinematic moments of inertia and excitation energies of the rotational bands of several low-lying two-quasiparticle high-K configurations in ^{252}No. In this nucleus, the rotational band built on the

1254 keV isomer has been observed recently with the assigned $K^\pi = 8^-$ configuration [41]. It is seen that the present calculations with both $K^\pi = 8^-$, $\frac{9}{2}^-[734] \otimes \frac{7}{2}^+[624]$ and $K^\pi = 7^-$, $\frac{9}{2}^-[734] \otimes \frac{5}{2}^+[622]$ two-neutron configurations give reasonable agreements with the experimental data. This provides useful information for experimental analyses. In the superheavy mass region, there have been many multi-quasiparticle high-K isomers observed experimentally [42–44].

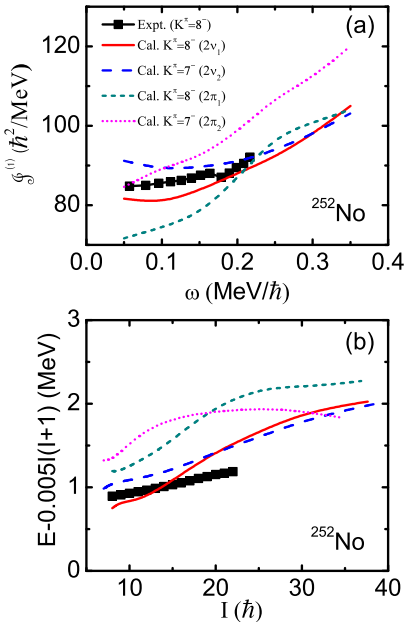

Fig. 3. (Color on-line) Calculated and experimental kinematic MoIs (a) and excitation energies (b) for the rotational band built on the 1254 keV isomer in ^{252}No. The excitation energies of the two-quasiparticle rotational bands were obtained by calculating their configuration-constrained TRSs. The experimental data are taken from Ref. [41]. The configurations are $2\nu_1$: $\nu\{\frac{9}{2}^-[734] \otimes \frac{7}{2}^+[624]\}$, $2\nu_2$: $\nu\{\frac{9}{2}^-[734] \otimes \frac{5}{2}^+[622]\}$, $2\pi_1$: $\pi\{\frac{7}{2}^-[514] \otimes \frac{9}{2}^+[624]\}$, and $2\pi_2$: $\pi\{\frac{7}{2}^-[514] \otimes \frac{7}{2}^+[633]\}$.

4. Summary

We have developed the configuration-constrained potential-energy surface calculation for multi-quasiparticle high-K states. An abundance of multi-quasiparticle high-K isomeric states in different mass regions have been investigated. The present calculations can well describe experimental excitation energies and deformations of high-K states. Further, we have

developed the configuration-constrained TRS calculation in which the paring correlation is treated by the particle-number-conserving method. As an example, we have shown configuration-constrained TRS calculations for the collective rotations of several two-quasiparticle high-K isomers in ^{252}No. The calculations are compared with available data, giving a good agreement between the calculations and data.

This research is supported by the National Key Basic Research Program of China under Grant No. 2013CB83440, the National Natural Science Foundation of China under Grants Nos. 11235001, 11320101004 and 11575007, the Open Project Program of State Key Laboratory of Theoretical Physics, Institute of Theoretical Physics, Chinese Academy of Sciences, China (No. Y4KF041CJ1), and the United Kingdom Science and Technology Facilities Council under grant No. ST/L005743/1.

REFERENCES

[1] P.M. Walker, G.D. Dracoulis, *Nature (London)* **399**, 35 (1999).
[2] P.M. Walker, G.D. Dracoulis, *Hyperfine Interact.* **135**, 83 (2001).
[3] F.R. Xu, P.M. Walker, J.A. Sheikh, R. Wyss, *Phys. Lett. B* **435**, 257 (1998).
[4] M.W. Reed *et al.*, *Phys. Rev. Lett.* **105**, 172501 (2010).
[5] F.R. Xu, E.G. Zhao, R. Wyss, P.M. Walker, *Phys. Rev. Lett.* **92**, 252501 (2004).
[6] H.L. Liu *et al.*, *Phys. Rev. C* **76**, 034313 (2007).
[7] S.W. Xu *et al.*, *Phys. Rev. C* **71**, 054318 (2005).
[8] S. Aberg, *Nucl. Phys. A* **306**, 89 (1978).
[9] F.R. Xu, P.M. Walker, R. Wyss, *Phys. Rev. C* **59**, 731 (1999).
[10] H.L. Liu, F.R. Xu, P.M. Walker, C.A. Bertulani, *Phys. Rev. C* **83**, 067303 (2011).
[11] A.N. Deacon *et al.*, *Phys. Rev. C* **76**, 054303 (2007).
[12] Yue Shi, P.M. Walker, F.R. Xu, *Phys. Rev. C* **85**, 027307 (2012).
[13] N. Alkhomashi *et al.*, *Phys. Rev. C* **80**, 064308 (2009).
[14] H.L. Liu, F.R. Xu, *Phys. Rev. C* **87**, 067304 (2013).
[15] F.R. Xu, P.M. Walker, R. Wyss, *Phys. Rev. C* **62**, 014301 (2000).
[16] J. Dudek, Z. Szymanski, T. Werner, *Phys. Rev. C* **23**, 920 (1981).
[17] F.R. Xu, W. Satula, R. Wyss, *Nucl. Phys. A* **669**, 119 (2000).
[18] F.R. Xu, *Chin. Phys. Lett.* **18**, 750 (2001).
[19] P.M. Walker, F.R. Xu, *Phys. Lett. B* **635**, 286 (2006).

[20] H.L. Liu, F.R. Xu, P.M. Walker, C.A. Bertulani, *Phys. Rev. C* **83**, 011303(R) (2011).
[21] H.L. Liu, F.R. Xu, P.M. Walker, *Phys. Rev. C* **86**, 011301(R) (2012).
[22] F.R. Xu, P.M. Walker, R. Wyss, *Phys. Rev. C* **65**, 021303(R) (2002).
[23] Y.H. Zhang *et al.*, *Phys. Rev. C* **68**, 054313 (2003).
[24] G.D. Dracoulis *et al.*, *Phys. Rev. C* **87**, 014326 (2013).
[25] G.D. Dracoulis *et al.*, *Phys. Lett. B* **720**, 330 (2013).
[26] Z. Podolyak *et al.*, *Phys. Rev. C* **66**, 011304 (2002).
[27] Z Podolyak *et al.*, *Phys. Lett. B* **491**, 225 (2000).
[28] G.D. Dracoulis *et al.*, *Phys. Lett. B* **635**, 200 (2006).
[29] C. Wheldon *et al.*, *Phys. Rev. C* **59**, R2334 (1999).
[30] C. Wheldon *et al.*, *Nucl. Phys. A* **652**, 103 (1999).
[31] C.S. Purry *et al.*, *Nucl. Phys. A* **672**, 54 (2000).
[32] F.R. Xu, R. Wyss, P.M. Walker, *Phys. Rev. C* **60**, 051301(R) (1999).
[33] W. Satula, J. Dobaczewski, W. Nazarewicz, *Phys. Rev. Lett.* **81**, 3599 (1998).
[34] X.M. Fu *et al.*, *Phys. Rev. C* **87**, 044319 (2013).
[35] X.M. Fu *et al.*, *Phys. Rev. C* **89**, 054301 (2014).
[36] J.Y. Zeng, T.H. Jin, Z.J. Zhao, *Phys. Rev. C* **50**, 1388 (1994).
[37] W. Nazarewicz, R. Wyss, A. Johnsson, *Nucl. Phys. A* **503**, 285 (1989).
[38] P. Moller, J.R. Nix, *Nucl. Phys. A* **536**, 20 (1992).
[39] Yue Shi, F.R. Xu, H.L. Liu, P.M. Walker, *Phys. Rev. C* **82**, 044314 (2010).
[40] C. Ardisson, J. Dalmasso, G. Ardisson, *Phys. Rev. C* **33**, 2132 (1986).
[41] B. Sulignano *et al.*, *Phys. Rev. C* **86**, 044318 (2012).
[42] S. Hofmann *et al.*, *Eur. Phys. J. A* **10**, 5 (2001).
[43] R.-D. Herzberg *et al.*, *Nature (London)* **442**, 896 (2006).
[44] H.B. Jeppesen *et al.*, *Phys. Rev. C* **79**, 031303 (2009).
[45] H.L. Liu, P.M. Walker, F.R. Xu, *Phys. Rev. C* **89**, 044304 (2014).
[46] Yue Shi, F.R. Xu, P.M. Walker, G.D. Dracoulis, *Phys. Rev. C* **85**, 064304 (2012).